中国物理学会
Chinese Physical Society

PAPER

A new cellular automaton for signal controlled traffic flow based on driving behaviors[*]

To cite this article: Yang Wang and Yan-Yan Chen 2015 *Chinese Phys. B* **24** 038902

A new cellular automaton for signal controlled traffic flow based on driving behaviors*

Wang Yang(王 扬) and Chen Yan-Yan(陈艳艳)[†]

Beijing Key Laboratory of Traffic Engineering, College of Metropolitan Transportation, Beijing University of Technology, Beijing 100124, *China*

The complexity of signal controlled traffic largely stems from the various driving behaviors developed in response to the traffic signal. However, the existing models take a few driving behaviors into account and consequently the traffic dynamics has not been completely explored. Therefore, a new cellular automaton model, which incorporates the driving behaviors typically manifesting during the different stages when the vehicles are moving toward a traffic light, is proposed in this paper. Numerical simulations have demonstrated that the proposed model can produce the spontaneous traffic breakdown and the dissolution of the over-saturated traffic phenomena. Furthermore, the simulation results indicate that the slow-to-start behavior and the inch-forward behavior can foster the traffic breakdown. Particularly, it has been discovered that the over-saturated traffic can be revised to be an under-saturated state when the slow-down behavior is activated after the spontaneous breakdown. Finally, the contributions of the driving behaviors on the traffic breakdown have been examined.

Keywords: cellular automata, signalized traffic systems, spontaneous traffic breakdown, driving behaviors

PACS: 89.40.Bb, 89.40.–a, 02.60.Cb
DOI: 10.1088/1674-1056/24/3/038902

1. Introduction

Issues of sustainability in the urban transportation system have become noticeable in a large number of cities worldwide. To efficiently manage the traffic in urban road networks requires a deep understanding of traffic flow operations and corresponding phenomena. To this end, researchers have proposed various cellular automaton (CA) models which have been shown to be a very promising alternative to reproduce and understand the complex behaviors of traffic flow. In 1992, Nagel and Schreckenberg[1] first proposed a stochastic cellular automaton model for vehicular traffic (known as the NaSch model) which can reproduce the basic features of traffic flow (e.g., spontaneous formation of jams). Since then, a considerable number of cellular automaton models have been developed to improve and extend the NaSch model, by incorporating aggressive acceleration,[2] velocity-dependent randomization,[3] comfortable driving,[4] anticipation behavior,[5] brake light effect,[6] a vehicle's honk effect,[7] decelerating damping effect,[8] safe driving,[9] etc.

In urban transportation systems, congestion is largely rooted in the traffic signal, which is an essential element for regulating the traffic flows of different directions. The existing CA models for the signal controlled traffic flow can be classified into two categories: one category focuses on the interaction between different directions of traffic flow at a signalized intersection based on two-dimensional traffic modelling and the other attempts to reproduce the traffic phenomena caused by the traffic signal using one-dimensional cellular

automata. As the CA model proposed in this paper aims to incorporate the driver's reactions when approaching the traffic light, a one-dimensional CA model is adopted and consequently related works are summarized here. Huang and Huang employed the NaSch model to investigate the synchronization effects among a set of traffic signals and found that the benefits of synchronization are obvious when the traffic density is low but marginal when traffic demand surpasses the saturated flow.[10] Neumanna and Wagner modified the NaSch model by introducing deceleration probability and analyzed the impact of traffic lights on travel time.[11] Jiang and Wu introduced a stopped time dependent randomization mechanism into the original NaSch model for the signal controlled intersection.[12] Varas *et al.* examined two control strategies for a sequence of traffic lights with a simple CA model in which the velocity of vehicles is limited to two values of 0 and 1.[13] In Ref. [14], the NaSch model was used to investigate the effects of four information feedback strategies on a scenario where two traffic lights were introduced to regulate vehicles to enter into an overlapped road link. Jan de Gier, et al.[15] developed a CA model for generic urban road networks and applied it to compare the effects of non-adaptive versus adaptive traffic signals for the vehicles obeying NaSch dynamics. Chowdhury and Schadschneider[16] developed a CA model for traffic flows in cities by combining the Biham–Middleton–Levine (BML) model and the NaSch model. They attempted to present the interactions between the traffic signal and vehicles and between vehicles by modifying the deceleration mechanism of the original NaSch model. Recently, Kerner *et al.*[17,18] used

†Corresponding author. E-mail: cdyan@bjut.edu.cn

the Kerner–Klenov–Wolf (KKW) model and investigated the dynamics of the signal controlled traffic and found the time-delayed traffic breakdown. The occurrence of the spontaneous traffic breakdown has been attributed to the phase transition from free flow to synchronized flow.[19,20]

From the above review, it is obvious that a few of the previous works have focused on modeling the driving behaviors in response to the traffic light, but most adopted the NaSch model (or similar models) to examine traffic flows under various traffic signal control strategies. As a result, some important phenomena may remain undercover due to the lack of adequate modelling for the signal-vehicle interaction. Furthermore, the previous research works did not take into account the effective region within which the vehicular movement is significantly affected by the traffic signal. In addition, driving behaviors are rather different for the moving and stopped vehicles during different signal phases, which are not separated in the previous works.

In order to overcome the aforesaid shortcomings, this paper proposes a CA model by incorporating the driving behaviors typically observed for the vehicles passing a traffic signal. A description on the developed model and traffic scenarios will be given in the next section. Following that, the primary experimental results will be presented and discussed in Section 3. The paper is concluded in Section 4.

2. Traffic scenario and model

2.1. The signalized traffic scenario

As this research primarily aims to model the driving behaviors induced by the traffic signal, a one-dimensional lattice is adopted to construct a single lane road segment with a traffic light which is operated in a fixed cycle manner. As shown in Fig. 1, the road segment consists of three sections, i.e., A, B, and C. Section A represents the part on which the vehicles are not affected by the traffic light, possibly due to the low visibility. The effective point is where the vehicular movement begins to be affected by the traffic signal operation. Sections B and C are separated by the traffic light, as different driving behaviors typically manifest in reality for the sections before and after a traffic light. All road sections are subdivided into a number of cells with the same length. Each cell is either empty or occupied by one vehicle travelling with a discrete velocity ranging from $v_{\min}$ to $v_{\max}$. In this paper, it is assumed that the maximum permitted velocity $v_{\max}$ is the same for all sections. For simplicity, one type of vehicle and homogeneous driver are assumed in the following.
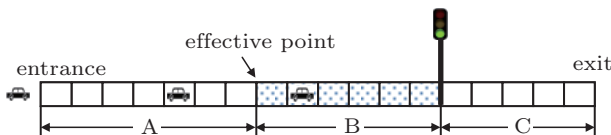

Fig. 1. (color online) The signal controlled traffic scenario.

2.2. The proposed model

To realize the dynamics for different road sections, the proposed model consists of two sets of rules, one for the normal sections (i.e., sections A and C) where only the reaction to the preceding vehicle exists and the other for the effective section (i.e., section B) where the vehicular movement is affected by both the preceding vehicle and the traffic signal.

Before explaining the rules, the definitions on the variables and parameters used in the model are given as follows. Let T_g, T_r, and T_y be the lengths of green, red and yellow phases, respectively, and $\bar{t}_g$, $\bar{t}_r$, and $\bar{t}_y$ be the remaining time for each phase. τ_i is the amount of time for which the vehicle i has been stopped. Let x_i and v_i denote the position and velocity, respectively, of vehicle i, and x_{i-1} and v_{i-1} be the position and velocity, respectively, of the vehicle ahead. $a_{\max}$ and $b_{\max}$ denote the maximum acceleration and deceleration per time step. In this paper, the vehicle is allowed to accelerate at a rate from 1 to $a_{\max}$ or decelerate at a rate from 1 to $b_{\max}$. Note that only an integer is allowed for the rates. Thus, the number of candidate acceleration rates n_a and the number of candidate deceleration rates n_b are equal to $a_{\max}$ and $b_{\max}$, respectively. While g_i denotes the gap from the vehicle to its predecessor, G_i is the distance from its current location to the stop line (i.e., the same position as the traffic light in this paper). p_{gm}, p_{gs}, p_{ym}, p_{ys}, p_{rm1}, and p_{rs}, denote the probabilities to be taken for the random deceleration for the moving and stopped vehicles during green, yellow, and red phases, respectively.

As the proposed model adopts limited acceleration and deceleration capabilities for vehicles, a full speed or a complete stop may require more than one time step of acceleration or deceleration. Thus, in order to determine the safe distances from the vehicle to its predecessor and the traffic light, two distances, $d^k_{\mathrm{veh}_i}$ and $d^k_{\mathrm{light}_i}$, are defined as

$$d^k_{\mathrm{veh}_i}(t) = g_i(t) + d_{\mathrm{lead}_{i-1}}(t) - d^k_{\mathrm{own}_i}(t), \qquad (1)$$

$$d^k_{\mathrm{light}_i}(t) = G_i(t) - d^k_{\mathrm{own}_i}(t), \qquad (2)$$

where

$$d_{\mathrm{lead}_{i-1}}(t) = \sum_{j=1}^{M_{i-1}} (v_{i-1}(t) - j b_{\max}),$$

$$d^k_{\mathrm{own}_i}(t) = \sum_{c=0}^{N_i} (v_i(t) + \delta_k - c b_{\max}),$$

$$(\delta_k \in \{-b_{\max}, \ldots, -1, 0, 1, \ldots, a_{\max},$$

$$k \in \{1, 2, \ldots, n_a + n_b + 1\})).$$

The distance $d^k_{\mathrm{veh}_i}(t)$ between two successive vehicles estimated in Eq. (1) takes into account the worst situation where the leading vehicle $i-1$ continually brakes at the maximum rate until it stops and the corresponding distance is defined as $d_{\mathrm{lead}_{i-1}}(t)$. The distance $d_{\mathrm{lead}_{i-1}}(t)$ together with the gap $g_i(t)$ is the total distance that vehicle i can travel before collision to the leading vehicle in the worst situation. $d^k_{\mathrm{own}_i}(t)$

is the distance when vehicle i attempts to change its velocity at the rate of δ_k ($\delta_k \in \{-b_{max}, \ldots, -1, 0, 1, \ldots, a_{max}\}$) at time step $t+1$ and then decelerate at the rate of b_{max} at the subsequent time steps until it stops. $M_{i-1} = \lfloor v_{i-1}(t)/b_{max} \rfloor$ ($\lfloor \rfloor$ denotes the floor function) is the number of time steps required by vehicle $i-1$ to come to a stop after a sequence of decelerations. On the other hand, the time steps required by vehicle i to come to a stop from $v_i(t) + \delta_k$ can be estimated by $N_i = \lfloor (v_i(t) + \delta_k)/b_{max} \rfloor$. Similarly, $d_{\text{light}_i}^k(t)$ in Eq. (2) denotes the remaining distance between the traffic light and the vehicle after it firstly alters its velocity at δ_k and then decelerates to zero at the maximum rate. Note that a non-negative value of $d_{\text{veh}_i}^k(t)$ or $d_{\text{light}_i}^k(t)$ indicates that the vehicle can travel with the desired velocity without traffic collision or violation and therefore the corresponding distance is called the safe distance in this paper.

1) Rules for the effective section Table 1 briefly summarizes the driving behaviors typically observed in reality for the vehicles approaching a traffic light and corresponding rules developed for the velocity update.

For the green phase, three rules have been designed for the velocity update so as to reflect the fast movement for the moving vehicles. First of all, the set of safe distances P is calculated according to Eq. (1) for δ_k ranging from $-b_{max}$ to a_{max}. Then, the velocity increment δ_{veh_i} that results in a minimum safe distance will be selected. This implies the intention of drivers to cross an intersection as fast as possible, provided the movement is safe. In addition, it has been found that many drivers decelerate without any exogenous reasons on the highway.[1] This may not be common for the signalized traffic, as more drivers would concentrate on driving when approaching an intersection where there are likely to be more traffic conflicts. Thus, a small probability should be assigned to the random deceleration (i.e., R3). Note that only a small deceleration rate (i.e., 1 cell/step^2) is allowed in R3 to reflect the fast movement.

Table 1. Typical driving behaviors and the corresponding velocity update rules for the vehicles on the effective section.

Phase	Moving vehicles ($v_i(t) > 0$)	Stopped vehicles ($v_i(t) = 0$)
Green	Fast movement	Slow-to-start at the beginning
	R1: Obtain $P = \{d_{\text{veh}_i}^k(t) \mid d_{\text{veh}_i}^k(t) \geq 0\}$ based on Eq. (1) with $-b_{max} \leq \delta_k \leq a_{max}$; R2: $v_i(t+1/2) \to \max(\min(v_i(t) + \delta_{\text{veh}_i}(t), v_{max}), 0)$, where δ_{veh_i} is the velocity increment that results in the minimum distance in P; R3: $v_i(t+1) \to \max\{v_i(t+1/2) - 1, v_i(t) - b_{max}, 0\}$ with p_{gm}.	R1: Obtain $P = \{d_{\text{veh}_i}^k(t) \mid d_{\text{veh}_i}^k(t) \geq 0\}$ based on Eq. (1) with $0 \leq \delta_k \leq a_{max}$; R2: $v_i(t+1/2) \to \max(\min(v_i(t) + \delta_{\text{veh}_i}(t), v_{max}), 0)$, where δ_{veh_i} is the velocity increment that results in the minimum distance in P; R3: $v_i(t+1) \to \max\{v_i(t+1/2) - a_{max}, 0\}$ with $p_{gs} = \min\{p_{max}, p_{gm} + 0.01\tau_i\}$.
Yellow	Slow-down if it cannot pass	Inch-forward to reduce the gap
	R1: Obtain $P = \{d_{\text{veh}_i}^k(t) \mid d_{\text{veh}_i}^k(t) \geq 0\}$ and $Q = \{d_{\text{light}_i}^k(t) \mid d_{\text{light}_i}^k(t) \geq 0\}$ based on Eqs. (1) and (2) with $-b_{max} \leq \delta_k \leq a_{max}$ if $G_i(t)/v_i(t) < \bar{t}_y$ or $-b_{max} \leq \delta_k \leq 0$ if $G_i(t)/v_i(t) \geq \bar{t}_y$; R2: $v_i(t+1/2) \to \max(\min(v_i(t) + \delta_{\text{veh}_i}(t), v_{max}), 0)$ if $G_i(t)/v_i(t) < \bar{t}_y$ or $v_i(t+1/2) \to \max(\min(v_i(t) + \delta_{\text{veh}_i}(t), v_i(t) + \delta_{\text{light}_i}(t), v_{max}), 0)$ if $G_i(t)/v_i(t) \geq \bar{t}_y$ (where δ_{veh_i} and δ_{light_i} are the velocity increments that result in the minimum distances in P and Q); R3: $v_i(t+1) \to \max\{v_i(t+1/2) - 1, v_i(t) - b_{max}, 0\}$ with p_{ym} if $G_i(t)/v_i(t) \geq \bar{t}_y$.	R1: Obtain $P = \{d_{\text{veh}_i}^k(t) \mid d_{\text{veh}_i}^k(t) \geq 0\}$ and $Q = \{d_{\text{light}_i}^k(t) \mid d_{\text{light}_i}^k(t) \geq 0\}$ based on Eqs. (1) and (2) with $0 \leq \delta_k \leq 1$; R2: $v_i(t+1/2) \to \max(\min(v_i(t) + \delta_{\text{veh}_i}(t), v_i(t) + \delta_{\text{light}_i}(t), v_{max}), 0)$ (where δ_{veh_i} and δ_{light_i} are the velocity increments that result in the minimum distances in P and Q); R3: $v_i(t+1) \to \max\{v_i(t+1/2) - 1, 0\}$ with p_{ys}.
Red	Slow-down in advance	Inch-forward to reduce the gap
	R1: Obtain $P = \{d_{\text{veh}_i}^k(t) \mid d_{\text{veh}_i}^k(t) \geq 0\}$ and $Q = \{d_{\text{light}_i}^k(t) \mid d_{\text{light}_i}^k(t) \geq 0\}$ based on Eqs. (1) and (2) with $-b_{max} \leq \delta_k \leq 0$; R2: $v_i(t+1/2) \to \max(\min(v_i(t) + \delta_{\text{veh}_i}(t), v_i(t) + \delta_{\text{light}_i}(t), v_{max}), 0)$ (where δ_{veh_i} and δ_{light_i} are the velocity increments that result in the minimum distances in P and Q); R3: if $v_i(t+1/2) > 0$, $v_i(t+1) \to \max\{v_i(t+1/2) - 1, v_i(t) - b_{max}, v_{min}\}$ where $v_{min} = 1$ with p_{rm1} and $v_{min} = 0$ with p_{rm0}.	R1: Obtain $P = \{d_{\text{veh}_i}^k(t) \mid d_{\text{veh}_i}^k(t) \geq 0\}$ and $Q = \{d_{\text{light}_i}^k(t) \mid d_{\text{light}_i}^k(t) \geq 0\}$ based on Eqs. (1) and (2) with $0 \leq \delta_k \leq 1$; R2: $v_i(t+1/2) \to \max(\min(v_i(t) + \delta_{\text{veh}_i}(t), v_i(t) + \delta_{\text{light}_i}(t), v_{max}), 0)$ (where δ_{veh_i} and δ_{light_i} are the velocity increments that result in the minimum distances in P and Q); R3: $v_i(t+1) \to \max\{v_i(t+1/2) - 1, 0\}$ with p_{rs}.

It is quite common that drivers stop focussing their attention on the signal while waiting at signalized intersections and may initiate other activities (e.g., making a call, playing with their mobile phone, reading newspapers, cleaning up windows, etc.), potentially resulting in a slow-to-start[7,21,22] when the light changes to green. Thus, this slow reaction is a typical behavior that the proposed model attempts to incorporate for a stopped vehicle. The first two rules are the same as those for the moving vehicles during green phase, except that only acceleration is allowed for the stopped vehicle (i.e., $0 \leq \delta_k \leq a_{max}$). However, the stopped vehicles may still be motionless with probability p_{gs} (in R3) which is dependent on the stopped time. We have adopted a linear increasing function of the stopped time as that in Ref. [12]. The probability p_{gs} should be larger than p_{gm}, as a stopped vehicle generally takes more time to start than a moving one due to the inertia of the vehicle or the reaction delay.[21]

A simple mechanism has been designed to govern the ve-

hicular motion during the yellow light. That is, a vehicle will move forward, if it can pass the traffic light location at the current velocity before the termination of the yellow light, and come to a stop, otherwise. Note that this mechanism implies an assumption that drivers know exactly the remaining time of yellow light. Such an assumption is not true in reality and the incomplete knowledge of yellow time often means that drivers are in a dilemma potentially resulting in red-running. However, the model proposed in this paper endeavors to avoid any traffic violations and this explains why such an unrealistic assumption is made in the model. The first rule is used to obtain two sets of safe distances P and Q based on Eqs. (1) and (2). Note that two sets of δ_k can be chosen depending on whether the vehicle can cross the intersection during the yellow phase. The first set ($-b_{\max} \leq \delta_k \leq a_{\max}$) is chosen if the vehicle can cross the intersection with its current velocity before the light changes to red. However, the second set ($-b_{\max} \leq \delta_k \leq 0$) indicates the vehicle needs to brake as it fails to cross the intersection within the remaining yellow time. Similarly, the velocity change is also arranged differently in R2 for the two situations. If the vehicle can cross the intersection before the onset of the red light, the influence of the traffic light is ignored. In the opposite situation, the distance to the traffic light has to be considered if a free traffic violation is desired. The vehicles that fail to cross the intersection during the yellow light may slow down in advance at a small rate of 1 cell/step^2. This behavior, called slowing-down in advance in this paper, is realized by R3 with probabilities p_{ym}. One should be aware of the fact that the behavior of slow-down in advance may result in a large gap between the vehicle and its predecessor. Unlike R3 for the green phase, the random deceleration is only applied to the vehicles that fail to cross the intersection during the yellow light. Such a constraint implies that the other vehicles pass through quicker during the yellow light than those during the green light.

During the yellow light, if a vehicle stops far from the stop line or its predecessor, three rules have been developed to help it inch forward to yield a closely spaced arrangement. However, it should be noted that a stopped vehicle cannot cross the intersection as its current velocity is zero. Thus, the influence of the traffic light is included when calculating the safe distances in R1 and modifying the velocity in R2. However, only a small acceleration rate is allowed (i.e., 1 cell/step^2), to reflect minor movement to gradually reduce the gap. The last rule presents that a few drivers would not like to move forward to reduce the gap possibly due to their laziness.

During the red light, a moving vehicle has to slow down and even stop to avoid the traffic violation and collision. Thus, the slow-down reaction is realized by setting $-b_{\max} \leq \delta_k \leq 0$. The second rule alters the velocity based on the safe distances obtained in the first rule. Subsequently, a proportion of moving vehicles (i.e., $v_i(t+1/2) > 0$) are subject to a further deceler-

ation process at a small rate of 1 cell/step^2, indicating these vehicles slow down in advance even though the deceleration is not necessary to avoid traffic violation and collision. To prevent a vehicle from stopping far from the traffic light or its predecessor, the minimum velocity is constrained to be a 1 cell/step with the probability p_{rm1}. However, a few drivers (e.g., new drivers) may initiate an over-deceleration, resulting in a stop far from the traffic light or its predecessor. Although such a phenomenon is rare, it is also considered in our model by assigning a small probability p_{rm0} (i.e., $p_{\text{rm1}} > p_{\text{rm0}}$) to R3 with $v_{\min} = 0$. The behavior of slow-down in advance keeps the vehicle moving for a longer time. Therefore, drivers can benefit from this behavior if their vehicles are still in motion after the onset of the green light, as the shorter time is generally required for a non-stopped vehicle to accelerate.[21]

The motion of a stopped vehicle in the red phase is controlled by the same rules as those for the stopped vehicles in the yellow light, but with different probability p_{rs} for R3. The probability p_{rs} primarily determines the number of vehicles that manifest a hysteresis reaction to reduce the gap to their predecessors.

To unify the rules listed in Table 1, one variable f is introduced to indicate the signal phase, with 1 being green, -1 red, and 0 yellow, respectively. Finally, an additional rule is appended to the unified three rules for the motion update. These four rules are used to simultaneously update the motions of all vehicles on the effective section.

R1 Safe distances. Calculate the value for $P = \{d_{\text{veh}_i}^k(t) | d_{\text{veh}_i}^k(t) \geq 0\}$ and $Q = \{d_{\text{light}_i}^k(t) | d_{\text{light}_i}^k(t) \geq 0\}$, where $d_{\text{veh}_i}^k(t)$ and $d_{\text{light}_i}^k(t)$ can be obtained according to Eqs. (1) and (2) with

$$\delta_{\max} = \begin{cases} a_{\max}, & \text{if } f = 1 \text{ or } (f = 0 \text{ and} \\ & v_i(t) > 0 \text{ and } G_i(t)/v_i(t) < \bar{t}_{\text{y}}), \\ 1, & \text{if } f \neq 1 \text{ and } v_i(t) = 0, \\ 0, & \text{otherwise,} \end{cases}$$

$$\delta_{\min} = \begin{cases} -b_{\max}, & \text{if } v_i(t) > 0, \\ 0, & \text{otherwise.} \end{cases}$$

R2 Speed modification. $v_i(t + 1/2) \rightarrow \max(\min(v_i(t) + \delta_{\text{veh}_i}(t), v_i(t) + \delta_{\text{light}_i}(t), v_{\max}), 0)$, where $\delta_{\text{veh}_i} = \arg\min\{P\} - \delta_{\min} - 1$ and

$$\delta_{\text{light}_i} = \begin{cases} \infty, & \text{if } f = 1 \\ & \text{or } (f = 0 \text{ and } v_i(t) > 0 \\ & \text{and } G_i(t)/v_i(t) < \bar{t}_{\text{y}}), \\ \arg\min\{Q\} - \delta_{\min} - 1, & \text{otherwise.} \end{cases}$$

R3 Random deceleration. $v_i(t+1) \rightarrow \max\{v_i(t+1/2) - \delta_{\text{rand}_i}(t), v_i(t) - b_{\max}, v_{\min}\}$ where

$$v_{\min} = \begin{cases} 1, & \text{with } p_{\text{rm1}} \text{ if } f = -1 \text{ and } v_i(t) > 0 \\ & \text{and } v_i\left(t + \frac{1}{2}\right) > 0, \\ 0, & \text{with } p, \\ v_i(t+1/2), & \text{otherwise,} \end{cases}$$

with

$$p=\begin{cases} p_{\text{gm}}, & \text{if } f=1 \text{ and } v_i(t)>0, \\ p_{\text{gs}}=\min\{p_{\max}, & \\ \quad p_{\text{gm}}+0.01\tau_i\}, & \text{if } f=1 \text{ and } v_i(t)=0, \\ p_{\text{ym}}, & \text{if } f=0 \text{ and } v_i(t)>0 \text{ and} \\ & G_i(t)/v_i(t)\geq \bar{t}_{\text{y}}, \\ p_{\text{ys}}, & \text{if } f=0, \text{ and } v_i(t)=0, \\ p_{\text{rm0}}, & \text{if } f=-1 \text{ and } v_i(t)>0 \\ & \text{and } v_i\left(t+\dfrac{1}{2}\right)>0, \\ p_{\text{rs}}, & \text{if } f=-1 \text{ and } v_i(t)=0, \end{cases}$$

$$\delta_{\text{rand}_i}(t)=\begin{cases} a_{\max}, & \text{if } f=1 \text{ and } v_i(t)=0, \\ 1, & \text{otherwise.} \end{cases}$$

R4 Motion update. $x_i(t+1)\rightarrow x_i(t)+v_i(t+1)$.

2) Rules for the normal sections At each discrete time step, all the vehicles on the normal sections are subject to a simultaneous motion update according to the following rules. The rules for the normal sections are similar to the rules for the vehicles moving on the effective section during a green light, except R3. The deceleration magnitude is either $a_{\max}$ or $b_{\max}$ according to whether the vehicle attempts to accelerate or decelerate in the preceding procedure.

R1 Safe distances. Calculate the value for $P=\{d^k_{\text{veh}_i}(t)|d^k_{\text{veh}_i}(t)\geq 0\}$ based on Eq. (1) with $-b_{\max}\leq \delta_k\leq a_{\max}$;

R2 Speed modification. $v_i(t+1/2)\rightarrow \max(\min(v_i(t)+\delta_{\text{veh}_i}(t),v_{\max}),0)$, where $\delta_{\text{veh}_i}=\arg\min\{P\}-b_{\max}-1$;

R3 Random deceleration. $v_i(t+1)\rightarrow \max\{v_i(t+1/2)-\delta_{\text{rand}_i}(t),v_i(t)-b_{\max},0\}$ with p_n, where

$$\delta_{\text{rand}_i}(t)=\begin{cases} a_{\max}, & \text{if } \delta_{\text{veh}_i}(t)>0, \\ b_{\max}, & \text{if } \delta_{\text{veh}_i}(t)\leq 0; \end{cases}$$

R4 Motion update. $x_i(t+1)\rightarrow x_i(t)+v_i(t+1)$.

3. Experiments

A set of simulations have been performed to examine what traffic phenomena the proposed model can reproduce, which driving behaviors respond to a specific traffic phenomenon, and how each parameter affects the traffic breakdown. Before presenting the results, the experiment settings are described firstly.

All the simulations have been initiated from an empty road which consists of a single lane of 200 cells (equivalent to 1km) with an open boundary. A traffic light is located at the 151th cell from the entrance and the effective section is 30 cells (150 m) in length. Vehicles with a maximum velocity of 3 cells/step (54 km/h with a time step of 1 s) enter into the system at a constant rate of 720 vehicles/h. The maximum rates of both acceleration and deceleration are assumed to be 10 m/s^2 in this paper. 110 s has been chosen for the signal cycle length, with $T_{\text{g}}=58$ s, $T_{\text{r}}=50$ s, and $T_{\text{y}}=2$ s. In all simulations, p_n has been set as 0.1 for section A, but 0 for section C to eliminate the influence of the randomization in the

downstream traffic on the upstream traffic of the intersection. Furthermore, the probability p_{rm0} has been fixed to be 0.01 whenever the slow-down behavior is activated.

3.1. Traffic phenomena reproduced

1) Time-delayed traffic breakdown Figure 2 presents the typical spatiotemporal pattern of traffic flow obtained from two independent runs with the slow-to-start behavior and the inch-forward behavior activated by setting $p_{\text{gm}}=0.1$, $p_{\max}=0.6$, $p_{\text{ym}}=0$, $p_{\text{ys}}=0$, $p_{\text{rm1}}=0$, $p_{\text{rm0}}=0.01$, and $p_{\text{rs}}=0$, respectively. The slow-down behavior is inactivated by allowing the velocity increment to vary in the range $-b_{\max}\leq \delta_k\leq a_{\max}$. The traffic flow is initially under-saturated, but it transits into the over-saturated traffic after the breakdown at approximately 1541th step (15th cycle) in Fig. 2(a) and 3631th step (33th cycle) in Fig. 2(b), respectively. By performing a number of independent runs, it can be found that the transition to the over-saturated traffic occurs after a random delay. This spontaneous traffic breakdown has been recently documented in Refs. [12], [17]–[20].
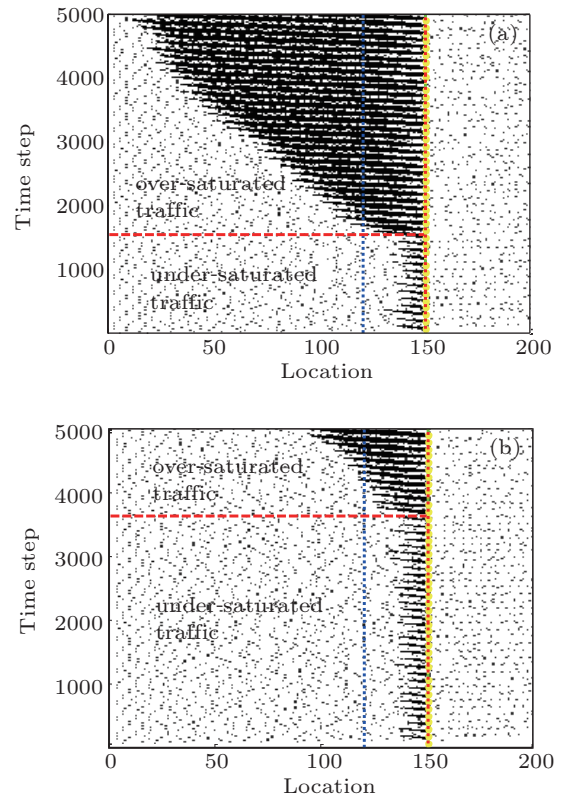

Fig. 2. (color online) The spatiotemporal pattern of traffic flow obtained from two independent runs. The effective section is bounded by the effective point and the traffic light whose locations are denoted by the two vertical lines from left to right. (a) One realization, (b) another realization.

In order to see the movement change before and after the breakdown in a microscopic way, the trajectories corresponding to the traffic shown in Fig. 2(a) are plotted for the two cycles just before and after the breakdown and shown in Fig. 3.

Before the traffic breakdown, the queue formed at the signal can be fully dissolved during the green phase and each vehicle closely follows its predecessor after the onset of the green signal, resulting in rapid queue dissolution. However, in the next green phase, the delayed start can be observed for a number of vehicles in the queue. This delayed start increases the stopped time and decreases the number of vehicles passing the traffic light accordingly. As the probability p_{gs} is linearly proportional to the stopped time, the increase of the stopped time will result in an increase of p_{gs} which is primarily responsible for the slow-start. In such way, the queue accumulatively extends step by step.
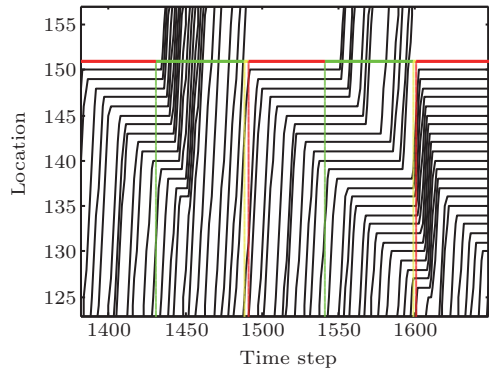
Fig. 3. (color online) Trajectories for the two cycles where the traffic transits from under-saturated state into over-saturated state. The upper horizontal line denotes the location of the traffic light.
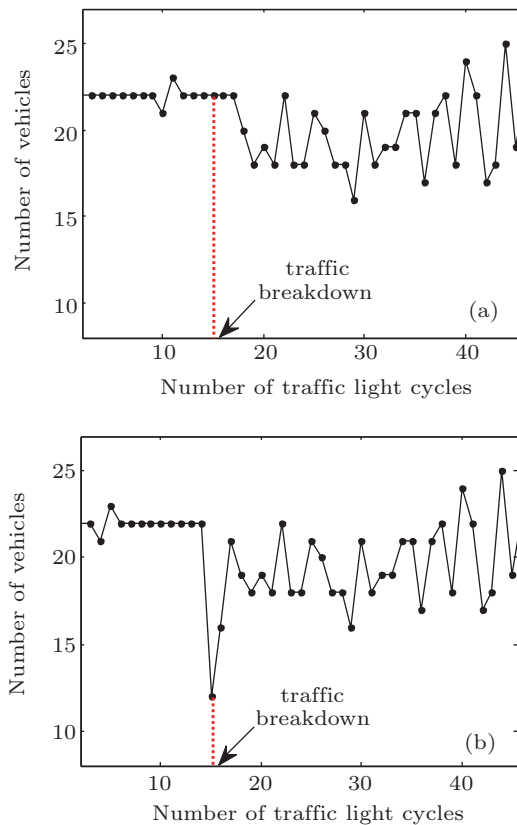

Fig. 4. (color online) Number of vehicles crossing the effective point (a) and the traffic light (b) in each traffic light cycle, corresponding to Fig. 2(a).

To further investigate the spontaneous breakdown, three parameters (i.e., number of vehicles, velocity, and time headway) for the traffic shown in Fig. 2(a) have been collected by using two virtual detectors located at the effective point and the traffic light, and the results averaged for each cycle are presented in Figs. 4–6.

A small variation on the number of vehicles crossing the effective point can be observed from Fig. 4(a) for the period before breakdown; the averaged number is approximately 22 (equivalent to 720 vehicles/h). On the contrary, the fluctuation becomes strong after the traffic transits to be over-saturated. Although the results shown in Figs. 4(a) and 4(b) have a similar pattern and the fluctuations are in the same order before and after the breakdown, there is a difference that a drop in the number of vehicles can be observed at the traffic breakdown cycle in Fig. 4(b) but the drop is delayed for a couple of cycles in Fig. 4(a). The drop in the number of vehicles passing the traffic light is largely resulted from the delayed start as evidenced by the averaged time headway presented in Fig. 6(b). The influence of the changes in the number of vehicles passing the traffic light will propagate upstream and therefore the number of vehicles passing the effective point will be affected with a time delay.
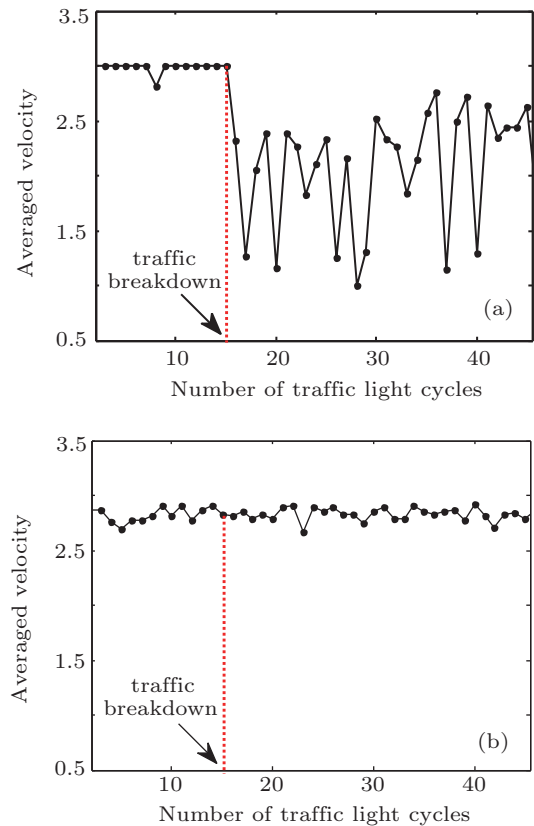

Fig. 5. (color online) Averaged velocity of the vehicles crossing the effective point (a) and the traffic light (b) in each traffic light cycle, corresponding to Fig. 2(a).

Figure 5(a) shows the averaged velocities when the vehicles crossing the effective point. In the under-saturated traffic,

the velocities averaged for each cycle is either maximum or near-maximum and the velocity variation is small. However, in the over-saturated traffic, the velocity decreases to almost 2 cell/step on average and the fluctuation becomes strong. On the other hand, the result in Fig. 5(b) implies that the breakdown has little influence on the averaged velocity of the vehicles crossing the traffic light and the fluctuation throughout the test period is smaller than that in Fig. 5(a). The small variation on the velocity indicates the outflow rate from the queue formed before the light turns to be green is constant and independent to whether the queue can be fully discharged during green time.
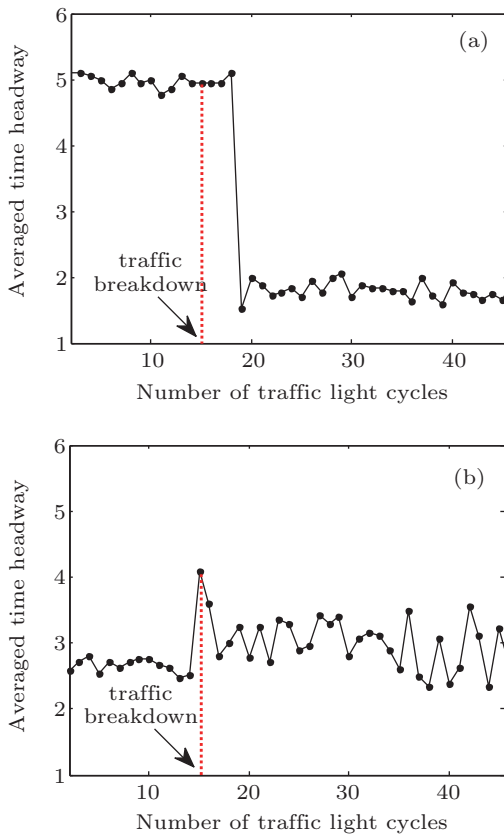

Fig. 6. (color online) Averaged time headway of the vehicles crossing the effective point (a) and the traffic light (b) in each traffic light cycle, corresponding to Fig. 2(a).

The time headway has been measured and averaged only for the vehicles that passed the effective point or the traffic light in each cycle. In other words, if a vehicle cannot cross the effective point or the traffic light during the current cycle, the time headway will not be included. In Fig. 6(a), before the breakdown, the averaged time headway is around 5 cells (25 m), approximately equivalent to the inflow rate of 0.2 vehicles/step. A sharp drop of the time headway can be observed after the breakdown for three cycles. The averaged time headway in the over-saturated traffic is around 2 cells (10 m). However, the situation is different when the vehicles are crossing the traffic light. At the breakdown cycle, the averaged time

headway is increased sharply, implying there is a considerable time loss due to the slow start. Consequently, the time loss causes a delay in the process of queue dissolution and some vehicles have to wait in front of the traffic light for another cycle (see Fig. 3). After the traffic breakdown, the fluctuation gradually becomes strong.
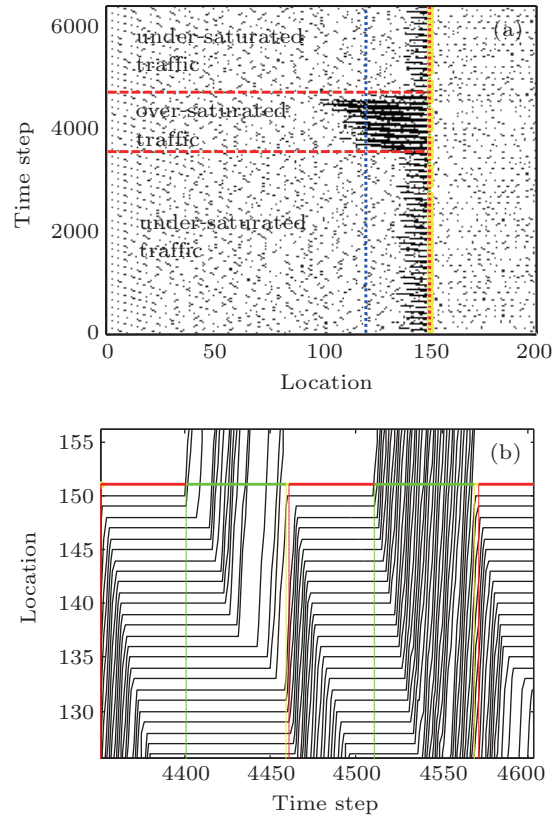

Fig. 7. (color online) The spatiotemporal pattern of traffic flow (a) and the trajectories for the two cycles just before and after the slow-to-start behavior is inactivated (b).

From Fig. 2(a), it can be seen that the upstream of the queue extends quickly into section A after the traffic breakdown. When the vehicle previously stopped in front of the effective point accelerates and crosses the effective point, the velocity, shown in Fig. 6(a), is generally small as it cannot accelerate to the maximum value within one time step. The vehicle stopped on section A will immediately accelerate with high probability (due to $P_n = 0.1$) as long as its front cell becomes free. This results in a small gap (headway is around 2 cells in Fig. 6(a)) between two successive vehicles.

To verify the influence of the slow-to-start behavior on the traffic breakdown, this behavior was initially activated but inactivated by setting $p_{gs} = p_{gm}$ after the traffic breakdown. However, during the test period, the inch-forward behavior is always on but the slow-down behavior off. Figure 7(a) shows the transition from the initial under-saturated state into the over-saturated state when the slow-to-start behavior is incorporated in the model, but the transition is reversed when the behavior is off. The trajectories shown in Fig. 7(b) correspond

to the traffic flow in Fig. 7(a) for the period when the slow-to-start behavior is switched off at the 4511$^{\text{th}}$ step. It is apparent that after the slow-to-start behavior is off the start delay is eliminated, resulting in a closely following pattern when the vehicles pass the traffic light.
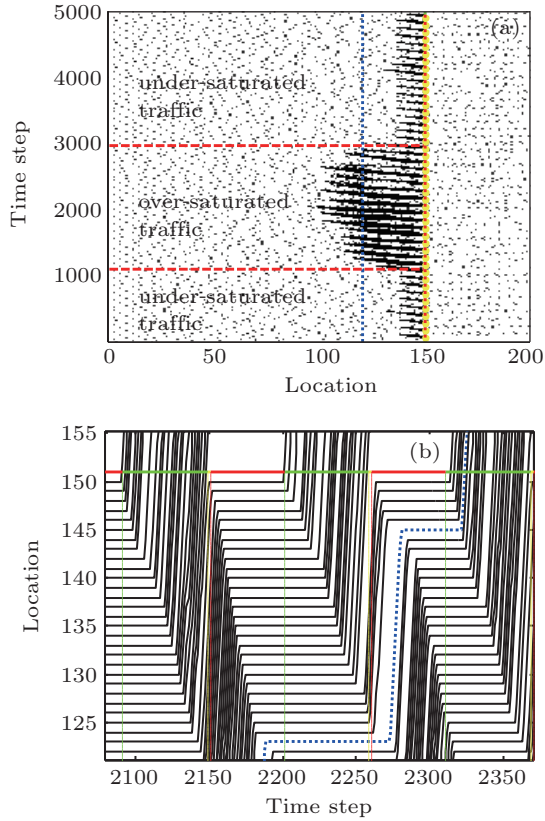

Fig. 8. (color online) The spatiotemporal pattern of traffic flow (a) and the trajectories for the two cycles just before and after p_{rs} is changed from 0 to 0.8 (b).

In addition, we have examined the influence of the inch-forward behavior on the traffic breakdown in the same way. The inch-forward behavior is isolated from the slow-to-start behavior by changing the inch-forward behavior (i.e., p_{rs} is changed from 0 to 0.8) but fixing the other during the test period. The traffic shown in Fig. 8(a) is initially under-saturated but changed to be over-saturated after the traffic breakdown. Then, p_{rs} is changed from 0 to 0.8 at the 2201$^{\text{th}}$ step and the queue begins to dissolve gradually. The trajectory marked as the dotted line in Fig. 8(b) indicates that, after p_{rs} is changed from 0 to 0.8, the vehicle originally stopped at the 123$^{\text{th}}$ cell is still motionless even though there is a big gap to the preceding vehicle during the red phase. After a while, the vehicle starts to move toward the traffic light and stops in front of the queue. This movement can reduce the queuing time for the vehicle and consequently the probability for the slow start. Then, the decrease of the slow start phenomenon can help the queue dissolution.

2) Dissolution of over-saturated traffic If the slow-down behavior is incorporated into the model, we have found that the traffic transits from over-saturation into under-saturation, promoting the queue dissolution. Figure 9(a) shows the traffic obtained when the slow-down behavior was activated by setting $p_{\text{rm0}} = 0.01$ and $p_{\text{rm1}} = 1$, after the over-saturated traffic lasted for eight cycles. Before activating the slow-down behavior, the traffic breakdown occurs at approximately the 1761$^{\text{th}}$ step (17$^{\text{th}}$ cycle), which was realized using the same setting as that in the last subsection with the slow-down behavior inactivated. Figure 9(b) shows the trajectories for the three cycles when the slow-down behavior was activated at the 2641$^{\text{th}}$ step (the 25$^{\text{th}}$ cycle). By a close observation on the movements for each red phase, it can be found that the velocity is relatively lower after the slow-down behavior was switched on. The low velocity prolongs the moving time and thus shortens the queueing time. As a result, the probability for the slow-to-start behavior is also reduced, as the probability is linearly dependent on the stopped time. In such a way, the queue can be gradually dissolved with the assistance of the slow-down behavior.
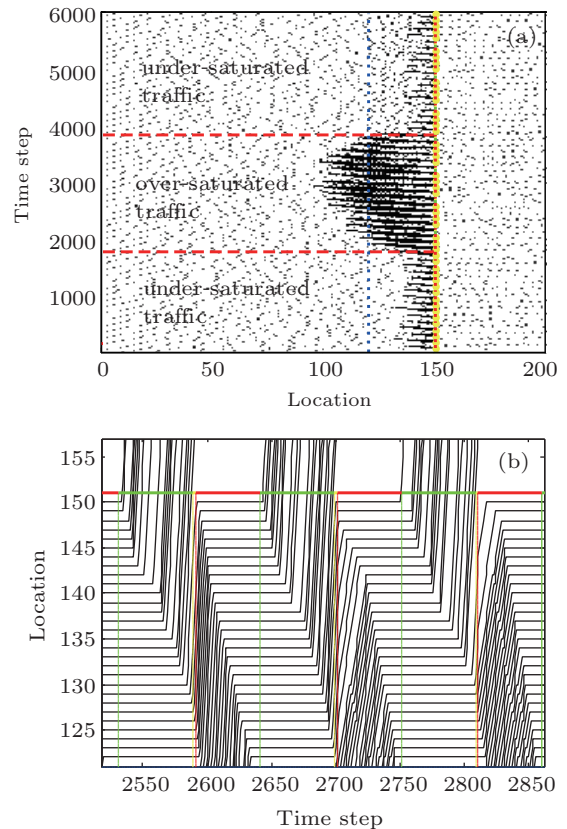

Fig. 9. (color online) The spatiotemporal pattern of traffic flow (a) and the trajectories for the three cycles when the slow-down behavior is activated at the 2641$^{\text{th}}$ cycle (b).

Figure 10 shows the number of vehicles passing the effective point and the traffic light in each cycle. The result shown in Fig. 10(a) indicates the number of vehicles driving through the effective points is around 22 on average and the variation is relatively small, in under-saturated traffic. After the traffic breakdown for six cycles, the number begins to fluctuate

strongly, with the maximum of 29 and the minimum of 17.

Figure 10(b) shows the number of the vehicles crossing the traffic light is relatively constant and 22 on average in under-saturated traffic. However, the number drops to 17 when the traffic breakdown occurs at the 17th cycle and the number reaches to the maximum when the traffic transits from the over-saturation to the under-saturation. The reason for the delayed fluctuation after the breakdown in Fig. 10(a) is that it takes some time to propagate the influence of the breakdown from the traffic light to the effective point.
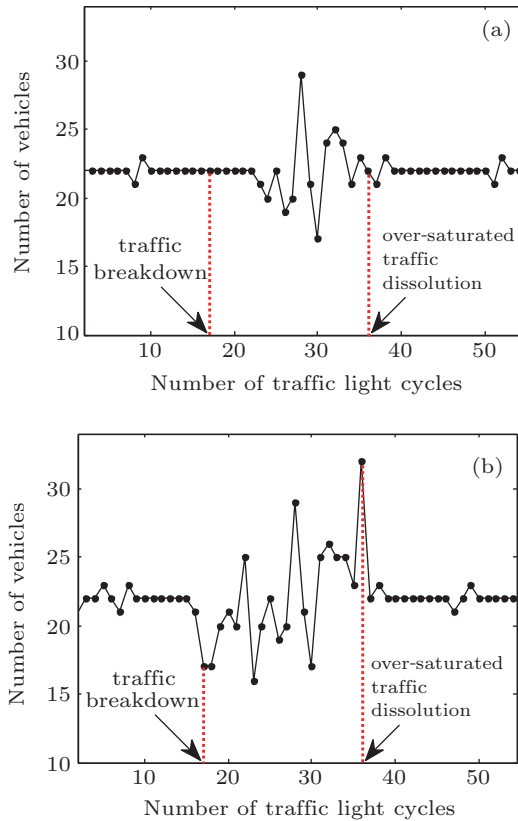

Fig. 10. (color online) Number of vehicles crossing the effective point (a) and the traffic light (b) in each traffic light cycle, corresponding to Fig. 9.

The velocities averaged for each cycle, when the vehicles crossing the effective point and the traffic light, are shown in Fig. 11. While figure 11(a) shows a down concave curve in general, the result in Fig. 11(b) fluctuates slightly. As shown in Fig. 11(a), the driving velocity is near to the maximum in under-saturated traffic, indicating a free flow around the effective point. The minimum value in over-saturated traffic is close to a 1 cell/step. The result in Fig. 11(b) indicates the vehicles passed the traffic light at high velocity and the fluctuation is weak through the test period.

The averaged time headway shown in Fig. 12(a) is approximately 5 cells for under-saturated traffic. After traffic breakdown for six cycles, the time headway goes down firstly, then varies slightly, and finally bounces up before the traffic transits into under-saturated traffic. On the contrast, there is no

apparent pattern in the result shown in Fig. 12(b), even though the fluctuation is generally stronger in the over-saturated traffic than that in the under-saturated traffics.
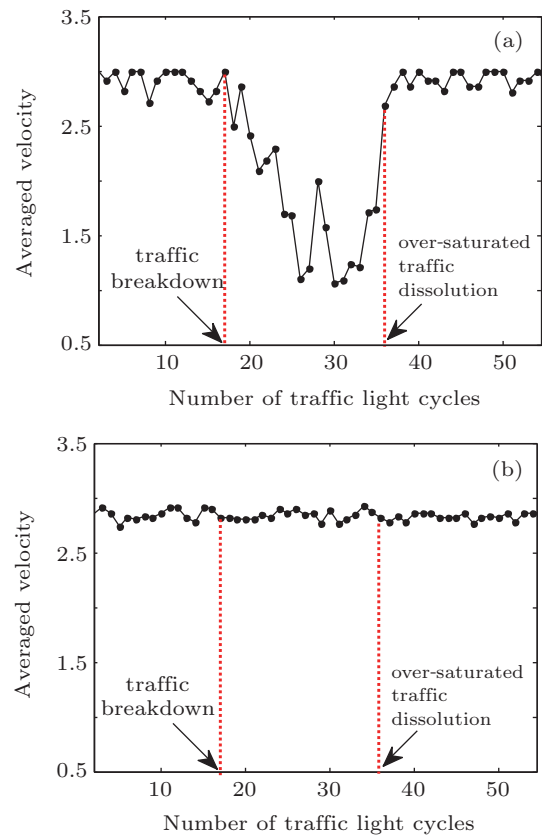

Fig. 11. (color online) Averaged velocity of vehicles crossing the effective point (a) and the traffic light (b) in each traffic light cycle, corresponding to Fig. 9.

The drop in the number after the breakdown shown in Fig. 10(b) can be explained by the slow-to-start effect as stated in the previous subsection. After activating the slow-down behavior, the vehicles will reduce their velocities during the red phases, even if it is not necessary to decelerate to avoid traffic violation and collision. With the slow-down behavior, the vehicles will take a longer time to reach the queue end, resulting in a reduced queuing time. As a result, the probability for the slow start will be reduced accordingly. As shown in Fig. 12(b), the small time headways around the transition from over-saturation to under-saturation indirectly show some evidence for the reduced slow start effect. This means that the queuing vehicles will start their movements with less delay and the number of vehicles passing the traffic light will be increased. Consequently, the slow-down behavior alleviates the tendency of the queue growing. The growing rate of the queue is effectively suppressed but the discharging rate is not altered, resulting in the queue shrinking step by step. This may account for why the slow-down behavior can help dissolve the over-saturated traffic.
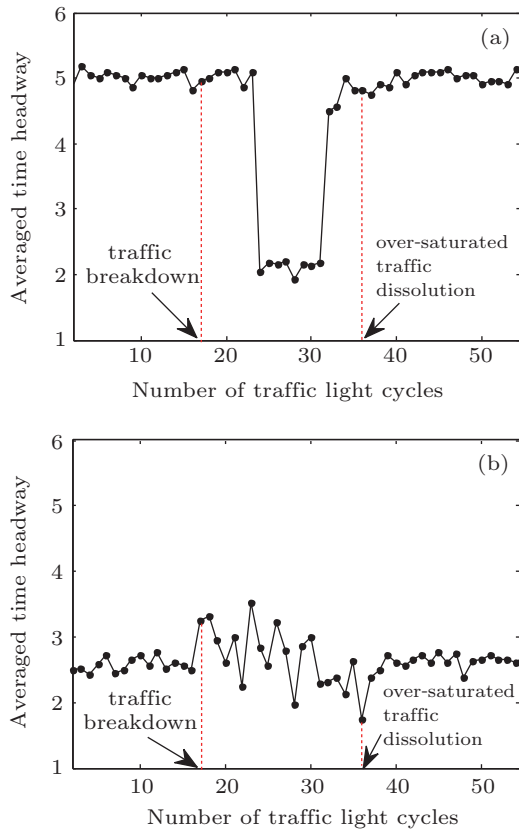
Fig. 12. (color online) Averaged time headway of vehicles crossing the effective point (a) and the traffic light (b) in each traffic light cycle, corresponding to Fig. 9.

3.2. Influence of driving behaviors on traffic breakdown

To evaluate the influence of different behaviors on traffic breakdown, we have performed a number of simulations by varying the probabilities. Figures 13(a) and 13(b) present the percentage and the averaged cycle at which the traffic broke down within 30 cycles and each has been averaged over 300 independent runs.

When examining the slow-to-start behavior, p_{max} has been firstly varied from 0.1 to 1 with an interval of 0.05, but p_{gm} fixed to be 0.1. Note that p_{max} should be larger in order to activate the slow-to-start behavior according to R3 for the vehicles on the effective section. By observing the percentage of traffic breakdown and the averaged breakdown cycle, it is clear that traffic breakdown never occurs during the test period when p_{max} is less than 0.55. When p_{max} increases from 0.55 to 0.7, the percentage increases gradually but the breakdown cycle decreases. When p_{max} is greater than 0.7, the percentage and breakdown cycle fluctuate slightly. Secondly, p_{gm} and p_{max} have been varied synchronously, so that the difference between them is always 0.5. In this way, the number of vehicles that manifest the slow-to-start behavior is mainly affected by the probability, p_{gm}. Note that p_{gm} is bounded at 0.5 when it increases from 0, as p_{max} reaches to 1 at that time. The result shown with the marker '+' in Fig. 13(a) indicates that the percentage of traffic breakdown is an increasing function of p_{gm}. However, the breakdown cycle decreases to 2 when

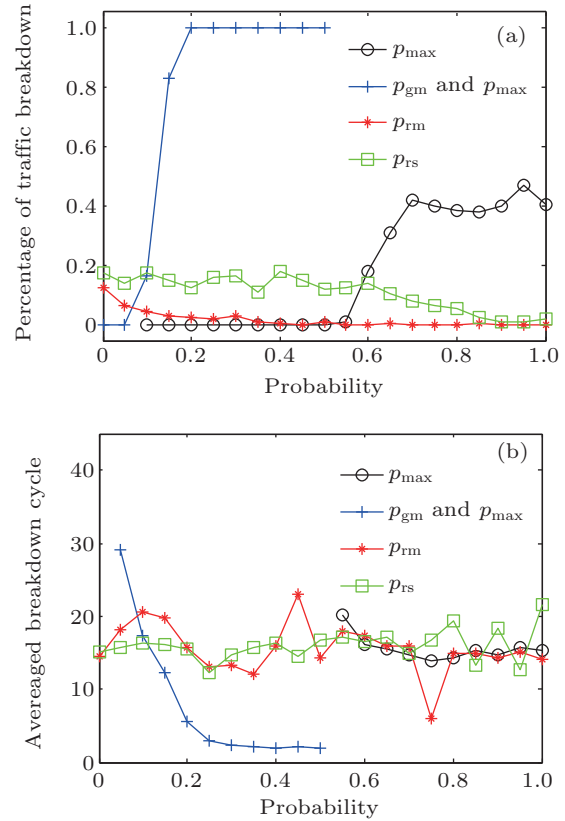p_{gm} is larger than 0.35. In short, the slow-to-start behavior potentially promotes traffic breakdown.

Fig. 13. (color online) Percentage of traffic breakdown (a) and the averaged breakdown cycle (b) for different probabilities.

Next, p_{rm1} has been varied but p_{rm0} fixed to 0.01 in order to generate the slow-down behavior with a different degree. The line with the marker '*' in Fig. 13(a) shows a decreasing tendency in the percentage of the traffic breakdown as p_{rm1} increases, indicating the probability of traffic breakdown can be reduced if the slow-down behavior is constantly reinforced. The result shown in Fig. 13(b) indicates that the traffic breakdown cycle is not significantly affected by p_{rm1}.

The final examination has been made by varying p_{rs} so as to realize the inch-forward behavior with a different degree. The result shown in Fig. 13(a) with the marker '□' indicates a general flat pattern when p_{rs} is less than 0.4 and a slow-decreasing pattern when p_{rs} is greater than 0.4. On the other hand, there is no apparent pattern for the breakdown cycle when p_{rs} increases. Note that the larger p_{rs} is, the more inactive is the inch-forward behavior. The result implies that traffic breakdown is likely to be affected negatively by the inch-forward behavior, even though the influence is not significant.

4. Conclusions

Various driving behaviors can be observed when vehicles approach and pass the traffic light. However, only a few driving behaviors have been considered in the existing models. To remedy this defect, the present work proposes a new model

which incorporates the typical driving behaviors and investigates the model dynamics based on a simulated road segment which consists of three sections.

Based on the simulations, the following can be concluded: first, a new CA model has been developed based on the traffic practice to reflect typical driving behavior; second, the proposed model can produce the time-delayed traffic breakdown and the dissolution of the over-saturated traffic phenomena; third, the driving behaviors that can potentially cause each macroscopic traffic phenomenon are identified; finally, the contributions of the microscopic behaviors to the macroscopic traffic breakdown are examined.

Nevertheless, only the primary investigation on the proposed model is presented in this paper and to conduct a more extensive exploration on the model dynamics certainly requires further research efforts.

References

[1] Nagel K and Schreckenberg M 1992 *J. Phys. I France* **2** 2211

[2] Ishibashi Y and Fukui M 1994 *J. Phys. Soc. Jpn.* **63** 2882

[3] Barlovic R, Santen L, Schadschneider A and Schreckenberg M 1998 *Eur. Phys. J. B* **5** 793

[4] Knospe W and Santen L 2000 *J. Phys. A* **33** L477

[5] Lárraga M E, Río J A and Schadschneider A 2004 *Phys. A: Math. Gen.* **37** 8753

[6] Tian J F, Jia N, Zhu N, Jia B and Yuan Z Z 2014 *Transp. Res. C* **44** 282

[7] Zheng L, Ma S and Zhong S 2011 *Physica A* **390** 1072

[8] Kokubo S, Tanimoto J and Hagishima A 2011 *Physica A* **390** 561

[9] Lárraga M E and Alvarez-Icaza L 2014 *Chin. Phys. B* **23** 050701.

[10] Huang D W and Huang W N 2003 *Phys. Rev. E* **67** 056124

[11] Neumann T and Wagner P 2008 *Eur. Phys. J. B* **63** 255

[12] Jiang R, Hu M B, Jia B and Gao Z Y 2014 *Comput. Phys. Commun.* **185** 1439

[13] Varas A, Cornejo M D, Toledo B A, Muñoz V, Rogan J, Zarama R and Valdivia J A 2009 *Phys. Rev. E* **80** 056108

[14] Tian L J, Huang H J and Liu T L 2009 *Chin. Phys. Lett.* **26** 078903

[15] Jan de G, Timothy M G and Omar R 2011 *J. Stat. Mech.* **4** 8

[16] Chowdhury D and Schadschneider A 1999 *Phys. Rev. E* **59** 1311

[17] Kerner B S 2011 *Phys. Rev. E* **84** 045102

[18] Kerner B S 2013 *Eur. Phys. J.* **102** 28010

[19] Kerner B S, Klenov S L and Schreckenberg 2014 *M J. Stat. Mech.* **3** 1

[20] Kerner B S 2014 *Physica A* **397** 76

[21] Tian J F, Yuan Z Z, Treiber M, Jia B and Zhang W Y 2012 *Physica A* **391** 3129

[22] Nishinari K and Takahashi D 2000 *J. Phys. A* **33** 7709